International Journal of Robotics and Control Systems
Vol. 3, No. 3, 2023, pp. 380-395
ISSN 2775-2658
http://pubs2.ascee.org/index.php/ijrcs

Technical and Economic Evaluation and Optimization of an Off-Grid Wind/Hydropower Hybrid System

Reza Alayi [a,1,*], Yaser Ebazadeh [b,2,*], Hossein Monfared [c,3], Salamollah Mohammadi-Aylar [d,4], Laveet Kumar [e,5], Alfian Ma'arif [f,6], Eskandar Jamali [g,7]

[a] Department of Mechanics, Germi Branch, Islamic Azad University, Germi, Iran
[b] Department of Computer Engineering, Germi Branch, Islamic Azad University, Germi, Iran
[c] Department of Mathematics, Germi Branch, Islamic Azad University, Germi, Iran
[d] Department of Agricultural Mechanization, Germi Branch, Islamic Azad University, Germi, Iran
[e] Department of Mechanical Engineering, Mehran University of Engineering and Technology, Jamshoro 76062, Pakistan
[f] Department of Electrical Engineering Universitas Ahmad Dahlan, Yogyakarta, Indonesia
[g] Department of Mechanics, Germi Branch, Islamic Azad University, Germi, Iran
[1] Reza.Alayi@iau.ac.ir; [2] yaser_ebazadeh@yahoo.com; [3] monfared.h@iaugermi.ac.ir; [4] s.m.aylar@gmail.com; [5] laveet.kumar@faculty.muet.edu.pk; [6] alfianmaarif@ee.uad.ac.id; [7] eskandarjamali76@gmail.com
* Corresponding Author

ARTICLE INFO

Article history
Received April 08, 2023
Revised May 10, 2023
Accepted June 07, 2023

Keywords
Clean Energy;
Wind turbine;
Hydropower turbine;
Economic modeling;
Ant Colony Optimization

ABSTRACT

Owing to global population growth, more fossil fuels are being used to meet the energy demand, which has led to increases in environmental pollution. Therefore, alternative sources such as renewable energy can be employed to meet some of the needs. Renewable energy has been criticized for its related problems such as downtime and high investment costs. In this study, a system was proposed to address these two problems by integrating wind and hydropower turbines, in Khalkhal, Ardabil, Iran as a case study. To appraise the system, an economic model was generalized, and an Ant Colony Optimization (ACO) method aiming to reduce investment costs was, implemented. The results show that to cover 100% of the required energy demand with a hybrid system of wind and hydropower turbines, the total cost of this system will be $ 202138. Also, the Cost of Energy (COE) per unit of generated power with the hydropower system, wind, and battery storage is gauged at 0.261 $/kWh. For the case study, to supply the required energy demand, 10 wind turbines and 23 kVA batteries, as well as a 14.6 kW hydropower turbine are required.

1. Introduction

The lack of electricity networks in remote areas and the cost of connection of these areas to national networks attributable to the undesirable geographical state of the region has led to the utilization of alternative energy sources, independent of the network [1, 2]. In recent years, diesel generators have been considered to supply the power required in these areas [3, 4]. However, the use of this generator has problems such as pollution caused by diesel fuel consumption [5], which elicits lung and respiratory diseases. Diesel fuel is considered a finite and non-renewable source, and in recent years, attention has been focused on reducing the consumption of fossil fuels and replacing it with clean and renewable energy [6–9]. The use of renewable energy, in turn, has problems such as the high cost of its construction and the dependence of its energy production on climate change [10,

11]. The main problems with using renewable sources are intermittent wind during the day and the lack of use of solar energy at night [11–14].

Hydropower plants have seen great attention. The cost of building the power plant is substantially low while providing uniform and usable electricity [15–17]. The energy obtained from the construction of hydropower plants is highly reliable among renewable energy sources and its construction cost is lower than others [18, 19]. However, due to the amount of energy demand, the small hydropower system alone is not able to supply this energy. It should be noted that hybrid renewable energy systems are a suitable solution for supplying electricity to remote areas [20–22]. Also, these systems are used to supply electricity to strategic and important areas such as border boundaries, offshore stations, telecommunication and television booster stations, etc.

Weather conditions, including river flow, wind speed, and air temperature usually change in different regions and places. Therefore, there are unstable shortages of generating electricity from small hydropower systems and wind turbines [23–25]. Due to efficiency and economic issues, designing a suitable sizing for hydropower and wind power generation systems with a battery is very important for the use of wind and hydropower renewable energy sources [26]. The size optimization method can help to achieve the lowest investment cost along with full use of a small hydropower system, a wind system, and a battery bank [27–29]. The following overview of relevant literature in this scope.

Ren et al. [30] analyzed the performance of a hybrid hydropower-photovoltaic-wind system and implemented multi-objective optimization for reducing the variance and maximum power generation through an owl search algorithm. Three climatic conditions were employed to analyze the efficiency of the hybrid system. In changing climates, the system continued to generate power. The Pareto front results demonstrated that the developed algorithm is the algorithm that comes closest to the Pareto front. As a result, improving the entire multi-objective integrated system was the most precise.

Lu et al. [31] applied an optimization model for the combination of a hydro-wind hybrid system. They asserted that coordinated operation augments the power output stability and generation profits by 4.66%. Tan et al. [32] evaluated the benefit and risks of the operation of the high-sized hydropower-wind-photovoltaic system and considered forecast uncertainty. They applied a case study in the Yalong River, China. They reported that the total power generation, power generation profit, and energy transmission line use efficiency all grew dramatically. They added that the detrimental impact of photovoltaic power and wind generation variability on the power grid can be mitigated.

Sterl et al. [33] conducted a study on decarbonizing the electricity mix via a hydropower plant integrated with wind power in Suriname. The results indicated that thermal power can be effectively supplanted by hydro-supported wind power systems. They reported that Suriname can achieve 20%–30% penetration of hydro-supported wind power. An innovative universal method to resolve the integrated systems module size was given by Zhang et al. [34] for the optimal arrangement of a grid-connected hydropower-wind-photovoltaic system. It was determined that the optimum capacity proportion of wind and PV for the integrated system was 0.256 and 0.744, individually. Zhao et al. [35] evaluated a PV-wind-hydro multi-energy system, relevant to Yalong River basin specifications. Their results demonstrated that the PV and wind power capacity rate is best gauged at 0.57:0.43.

In retrospect, in this study, a small hydropower system with a wind turbine is used as a hybrid system to generate and supply the electricity in a remote village in Ardabil, a northwestern province of Iran. Information about the river discharge located in this village and also the intensity of the wind in the region is obtained from the Iran power plant investment company (SANA) and included in the modeling of the combined system. In addition, an approximate reliability model is used in this paper. The purpose of this work is to investigate the responsiveness of the proposed system to provide reliable power required by rural consumers during the year, and fills a literature gap within this scope.

2. Method

2.1. Combined System Structure

A small hydro and wind power generation system is comprised of a combination of hydroelectric generators, wind turbines, battery banks, inverters, controllers, and other necessary tools and cables. A schematic diagram of an energy hybrid system is shown in Fig. 1. In this system, small hydropower and wind turbines operate together for meeting the load demand. The generating power after meeting the load demand feeds the battery until the charge is complete. On the other hand, when energy is scarce, the battery will discharge its stored energy to help with small hydropower and wind turbines to meet load demand until it runs out of power. In other words, for predicting the performance of hybrid systems, first, it is necessary to model each of the components of the system (small hydropower, wind, and battery) and then their combination can be assessed to meet the load demand. Small hydropower, wind turbine, battery bank, and dump load are based on the following priority: the supply of power in the first place, then the battery bank, and finally the dump load are in demand. Electricity generated by small hydropower and wind turbines is regulated by a voltage regulator and when there is a shortage of load electricity generated by an additional hybrid system is stored by battery banks. But as known, the amount of electricity generated by the small hydropower turbine and wind energy in a hybrid system depends on the flow of river water and wind speed. One source of energy is at a lower level of production while the other is usually at a higher level of production. For example, in winter, the wind speed is generally at a high level while the river flow is at a low level. It is should be addressed that the simultaneous utilization of multi-generation sources generally augments the reliability of load demand [36].

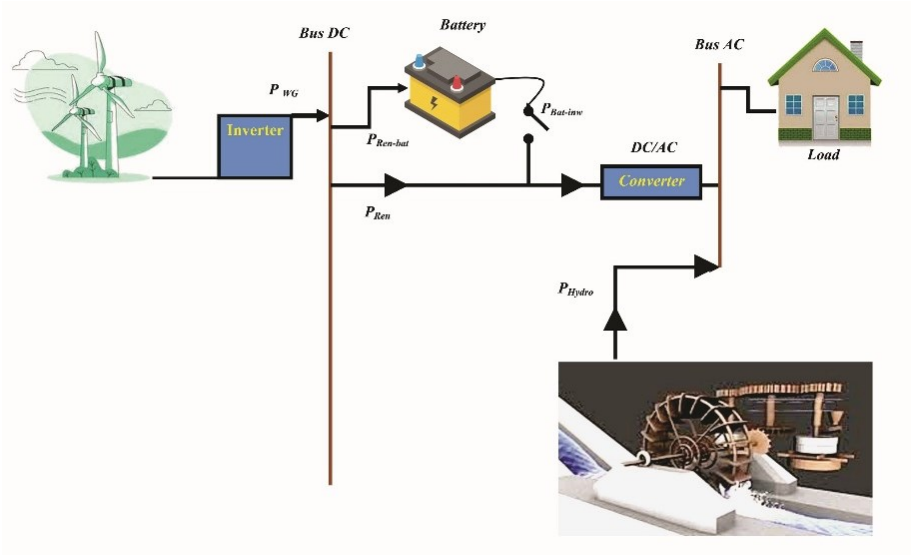

Fig. 1. Small hydropower turbine-wind turbine hybrid system with a battery storage system

2.2. Hydropower System Model

For the desired location, two main parameters of waterfall height and water flow were measured at 5 m and 187 L/s (0.187 m^3/s), respectively. The available potential of electric power from water sources is equal to 7.4375 kW, which is obtained from the following equation [37]:

$$P_{Total} = p_h \times \eta_t \times \eta_g \quad (1)$$

where η_t, η_g, and p_h are turbine efficiency, generator efficiency, and hydraulic power, respectively. The output power of the theory according to the location of the turbine is obtained by the following equation [38]:

$$P_h = C_W \times \rho_e \times g \times h_f \quad (2)$$

In the above relation, C_W is the density of water, ρ_e is the electric discharge coefficient, g is the acceleration of gravity and h_f is the height of the waterfall. Kaplan-type turbines (small size and higher speed) can be used due to the topology and hydrological properties of the area [38]. According to the type of turbine and its technical specifications, the turbine efficiency is considered to be 90%. Owing to its variable rotor speed characteristic compared to a synchronous generator, an induction generator is employed to produce variable speed [39, 40]. Generator efficiency is considered to be above 90%. The main specifications of the generator are tabulated in Table 1.

Table 1. Technical specifications of the generator

Type	Induction Generator
Nominal power (kW)	7.5
Efficiency (%)	90
Frequency (Hz)	50
Power factor	0.8
Synchronous speed (rpm)	1500
Rotor speed (rpm)	1560
Rotor inertia	0.02

2.3. Wind Turbine Model

Three main factors can govern the output of a wind energy conversion system (WECS), which are the output power curve (obtained by aerodynamic efficiency, η_m mechanical transmission, and η_g electrical conversion efficiency). From a selected wind turbine, wind speed distribution from a selected installation site, and wind tower heights are extracted. It should be noted that choosing a suitable model to simulate the output power is very important. The most simple model for simulating the output power of a turbine can be described by [41]:

$$P_w(v) = \begin{cases} P_R.\dfrac{v - v_C}{v_R - v_C}(v_C \le v \le v_R) \\ P_R(v_R \le v \le v_F) \\ 0(v \le v_C and v \ge v_F) \end{cases} \quad (3)$$

where P_R is the relative electrical power, v_C is the low cut-off wind speeds, v_R is the relative wind speed, and v_F is the high cut-off wind speed. In small-scale wind turbines, low cut-off wind speeds are comparatively small, and wind turbines can function straightforwardly even when wind speeds are not too high. The important point is that changes in wind speed with altitude, affect both the evaluation of wind benefits and the wind turbine design. In general, two mathematical models are utilized for modeling vertical wind speed profiles in similar areas. The first is the log law, which is based on the boundary layer flow in fluid mechanics. The second is the law of power, broadly employed by researchers. Generally, the power law characterizes a simple model for the speed profile of vertical wind. The fundamental form of this method is given as:

$$\frac{\upsilon}{\upsilon_r} = \left(\frac{z}{z_r}\right)^{\alpha} \quad (4)$$

where υ is the wind speed at the height of the hub Z (m/s) (height of the turbine above ground) and υ_r is wind speed measured at reference height. The α changes increase with parameters such as day, season, nature of the earth, temperature, wind speed, and assorted combined mechanical and thermal parameters. The value 1.7 is commonly used whenever no specific information from the site is available.

2.4. Battery Model

The lead-acid type is set for the battery bank, which is employed for storing surplus electrical energy for regulating the voltage of the system and for supplying power to load at lower wind speeds. These batteries operate under very precise conditions. Therefore, it is problematic for predicting the

time's energy will be supplied to or extracted from the battery. Parameters such as charge current, charge efficiency, inductor discharge, and battery capacity affect battery behavior. Most battery models focus on three different parameters, such as battery state of charge (SOC), floating voltage, and battery life.

2.4.1. Battery SOC

As already known, energy is stored in the battery when the wind turbine generated power and hydropower is more than the load. Energy is extracted from the battery when the generating power cannot meet the load needs, and when the power output by both the wind turbine and the hydropower turbine is inadequate and the storage is exhausted, the load will be cut off. The battery capacity, alike all chemical processes, relies on temperature. Generally, the battery capacity changes are defined by addressing the temperature coefficient δ_C:

$$C'_{bat} = C_{bat}(1 + \delta_C(T_{bat} - 298.15)) \tag{5}$$

In this equation, C'_{bat} is the operating battery capacity at a battery temperature of T_{bat} [K], C_{bat} is the nominal or relative battery capacity (given by the manufacturer), $\delta_C = 6\%$ is the temperature coefficient in degrees, or else it is given by the manufacturer. To find the true battery SOC, having the initial SOC, current discharging, or charging time is vital. Nevertheless, approximately many storage systems aren't ideal and losses take place during charge and discharge and throughout periods of storage. Battery SOC at t+1 can be calculated through the:

$$SOC_{(t+1)} = SOC_{(t)}\left(1 - \frac{\sigma\Delta t}{24}\right) + \frac{I_{bat}(t)\Delta t\eta_{bat}}{C'_{bat}} \tag{6}$$

where σ is the amount of self-discharge that relies on the battery health and total charge and the suggested value is 0.2%/day. It is problematic for measuring separate discharge and charge efficiencies; thus, manufacturers typically define a specific efficiency limit. Regularly, the battery charge efficiency is equivalent to the adjusted efficiency and the discharge efficiency is set as one. Battery current in the hybrid system at time t can be described by:

$$I_{bat}(t) = \frac{p_{pv}(t) + P_{wt}(t) - P_{ACload}(t)/\eta_{inverter} - P_{DCload}(t)}{V_{bat}(t)} \tag{7}$$

The efficiency $\eta_{inverter}$ is found based on the load profile and inverter characteristics are considered to be 92%. For simplicity, we assume that the wind turbine has a DC output, so it is not necessary to use a rectifier .Nonetheless, if a wind turbine is intended for being connected to an AC network, rectifier losses must be taken into account for a portion of the wind energy that goes from AC to DC.

2.4.2. Battery Floating Charge Voltage

The battery floating charge voltage response is modeled under both the charge and discharge conditions via the equation-fit technique, whereby models the battery as a black box and defines the floating charge voltage through a polynomial in periods of battery SOC and current. The battery floating charge voltage of the (V'_{bat}) can be calculated by:

$$V'_{bat} = A \times (SOC)^3 + B \times (SOC)^2 + C \times SOC + D \tag{8}$$

In other words, the temperature coefficient δ_V is used to calculate the effects of temperature on battery voltage predictions:

$$V_{bat} = V'_{bat} + \delta_V(T_{bat} - 298.15) \tag{9}$$

where V_{bat} is the calibrated battery voltage, thereby the temperature effects are taken into account. For the temperature range considered by the battery, the temperature coefficient δ_V is considered constant at -4mV/C in cell V_2. In the previous equation, the parameters A, B, C, and D are battery current functions that can be obtained from the quadratic polynomial equations as follows [42]:

$$\begin{bmatrix} A \\ B \\ C \\ D \end{bmatrix} = \begin{bmatrix} a_1 & a_2 & a_3 \\ b_1 & b_2 & b_3 \\ c_1 & c_2 & c_3 \\ d_1 & d_2 & d_3 \end{bmatrix} \begin{bmatrix} I^2 \\ I \\ 1 \end{bmatrix} \tag{10}$$

The parameters can be calculated via the least-squares method through equations expressed with battery performance data (given by the manufacturer). The parameters used for the battery are defined as:

$$\begin{bmatrix} a_1 & a_2 & a_3 \\ b_1 & b_2 & b_3 \\ c_1 & c_2 & c_3 \\ d_1 & d_2 & d_3 \end{bmatrix} = \begin{cases} \begin{bmatrix} -0.0015 & 0.05509 & 0.15782 \\ 0.00165 & -0.05758 & -0.39049 \\ -0.00024 & 0.01018 & 0.52391 \\ -0.00014 & 0.00795 & 1.86557 \end{bmatrix} \\ \begin{bmatrix} 0.00130 & 0.00093 & 0.03533 \\ -0.00201 & -0.00803 & -0.08716 \\ 0.00097 & 0.00892 & 0.22999 \\ -0.00021 & -0.00306 & 1.93286 \end{bmatrix} \end{cases} \tag{11}$$

Here, I > 0 indicates the battery charge process and I < 0 indicates the battery discharge process.

2.4.3. Limitations of Battery Simulation

Battery SOC is used as a design variable to control overcharge and discharge protection. Overcharging may take place when the ballast power is generated by the hybrid system or when there is a low load demand. Herein, when the battery SOC reaches the maximum value $SOC_{max} = 1$, the control system interferes and halts the charging process. In other words, if the charging mode is reduced to a minimum level $SOC_{min} = 1 - DOD$, the control system shuts off the load.

2.5. Economic Model

2.5.1. ACS Economic Model

In the economic method, grounded on the concept of the annual cost of the system (ACS), the annual cost of the system is combined with the annual marginal cost $of\ C_{acap}$, the annual replacement cost $of\ C_{arep}$, and the annual maintenance cost of C_{amain}. For this model, five important parts are considered: hydropower, wind turbine, battery, and other parts are equipment that is not included in the design variables. ACS can be expressed by:

$$\begin{aligned} ACS = C_{acap}(PV + Wind + Bat + Tower + Others) \ + C_{arep}(Bat) \\ + C_{amain}(Wind + Bat) + Tower + Others \end{aligned} \tag{12}$$

2.5.2. Annual Investment Cost

The annual investment cost of each combination of the hybrid system is known as the installation cost. The investment cost can be calculated as follows:

$$C_{acap} = C_{cap} CRF\left(i - Y_{proj}\right) \tag{13}$$

where Y_{proj} is the life time combined (year), CRF is the capital recovery factor that is a rate for calculating the present value of one year (a series of equivalent annual cash flows). The CRF is calculated using the following equation [43, 44]:

$$CRF\left(i.Y_{proj}\right) = \frac{i.(1+i)^{Y_{proj}}}{(1+i)^{Y_{proj}} - 1} \tag{14}$$

The annual real interest rate i is given by the following equation that is pertinent to the nominal interest rate i', and the annual inflation rate f:

$$i = \frac{i' - f}{I + f} \tag{15}$$

2.5.3. Annual Replacement Cost

The annual replacement cost is the annual amount of all replacement costs incurred during the life of the project. In the proposed hybrid system, only the battery necessities of being periodically supplanted during the project [45]:

$$C_{arep} = C_{rep}.SFF\left(i, Y_{rep}\right) \tag{16}$$

where C_{rep} is the cost of replacing the battery, Y_{rep} is the lifespan of the battery (years), and SFF is the meeting factor, equivalent to a rate for calculating the future value of a series of annual cash flows:

$$SFF\left(i, Y_{rep}\right) = \frac{i}{(I+i)^{Y_{rep}} - 1} \tag{17}$$

2.5.4. Maintenance Costs

The maintenance cost of the system is calculated by considering the given inflation rate:

$$C_{amain}(n) = C_{amain}(1+f)^n \tag{18}$$

In this equation, $C_{amain}(n)$ is the nth-year maintenance cost. The lowest ACS is considered one of the optimal combinations that can ensure the required power supply reliability.

2.5.5. LCE Economic Model

An optimal integration of the hybrid wind and hydropower turbine energy system must be found, from both reliability and economic standpoints [46]. Based on the studied wind and hydropower hybrid power generation system, the energy leveling cost is expressed as the total cost of the hybrid system over the energy supplied. The economic model can be divided into three parts (wind turbine, hydropower turbine, and battery bank):

$$LCE = \frac{\sum_{i=1}^{n} (CO/y_i)}{E_{an}} = \frac{CO_{hydro}/Y_{hydro} + CO_W/Y_W + CO_{Bat}/Y_{Bat}}{E_{an}(\gamma, \beta, h)} \tag{19}$$

That LCE is the Levelized cost of energy. In this equation, CO_{hydro}, CO_{Bat}, and CO_W are the total investment cost and maintenance cost in the lifespan of hydropower, battery, and wind power generation systems, respectively, CO_{Bat} is the total investment cost and maintenance cost in the lifespan of the battery bank, Y_{hydro} and Y_W are the lifespans of a hydropower and wind system, respectively, Y_{Bat} is the life of the battery bank and $E_{an}(\gamma, \beta, h)$ is the annual energy that is supplied by the wind-hydropower hybrid system. The combination with the lowest LCE is taken as the optimal combination that ensures the required reliability of the power supply.

2.6. Ant Colony Optimization (ACO)

A promising source of repetition is the collective behavior of ants in nature. To find food, they randomly search the space around their nest, and when they find food, according to the type and quality of food, they bring some of it to their nest, and when they return, they secrete a pheromone. The ants come to the food and as the number of ants increases, the amount of pheromone secreted increases, and the shortest possible path is identified. Using the ant colony algorithm (ACO), the longest and shortest paths from each node to another node within the network can be optimized, as well as the effect of activity dependence on resource movement. Since the ACO algorithm attempts to mimic the behavior of real ants using a simulation process, a probability function is used to describe the path. The probability of accessing point j from point i (transfer probability) is calculated according to the following formula:

$$P_{ij} = \begin{cases} \dfrac{\tau_{ij}^{\alpha} \cdot \eta_{ij}^{\beta}}{\sum_{httabuK} \tau_{ij}^{\alpha} \cdot \eta_{ij}^{\beta}}, & if\, j \notin tabuK \\ 0 \end{cases} \tag{20}$$

In this formula, τ_{ij}^{α} is the amount of pheromone chemical in points (i,j), which is also called the ant sense. η_{ij}^{β} is the ratio of points of view (i,j) which is called the ant eye and is a heuristic of the problem and is defined as $\eta_{ij} = 1/d_{ij}$, where d_{ij} is the distance between two nodes i and j. α and β are compatible parameters, introducing the importance of the path against the aspect ratio when choosing the next point to move. Finally, *tabuK* is the list of nodes visited in the current path, called ant memory. Fig. 2 shows the flowchart of the ant colony algorithm.

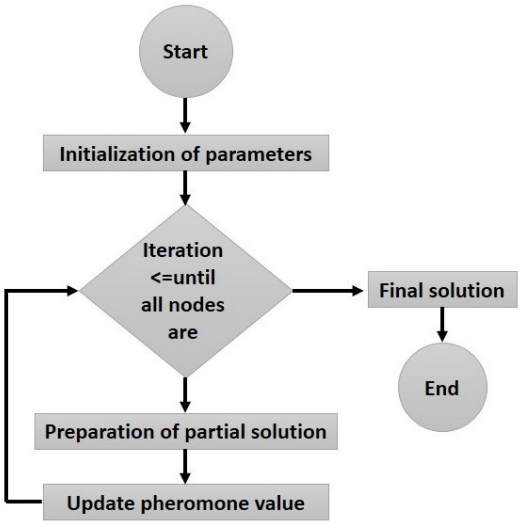

Fig. 2. Flowchart of the ant colony algorithm

2.6.1. Objective Functions

In the proposed method, the output of the optimal measurement algorithm is the number of wind turbines, batteries, and hydropower turbines [47]. These values must be optimized so that the 20-year cost of the system is ultimately equal to the minimum possible value. The total cost of the system $NPC(x)(\$)$ is equal to the total investment costs $C_c(x)(\$)$ and maintenance costs $C_m(x)(\$)$:

$$NPC(S) = N \times \left(Capital\ cost + (replacement\ Cost \times k)\right) + \left(Operation\&Maintenance\ Cost \times \frac{1}{CRF(ir,\pi)}\right) \quad (21)$$

In which:

$$S = \{hydro, WG, Batt\} \quad (22)$$

S vector includes the amount of power that can be extracted from a hydroelectric generator, wind turbine, batteries, inverter power, the number of charger batteries, and the optimal installation height of wind turbines. The CRF and K values are the payback ratio and the present value of the payment, respectively, which are calculated by the following equations:

$$y = \begin{cases} \left[\frac{R}{L}\right] - 1 : \text{if } R \text{ is dividable to } L \\ \left[\frac{R}{L}\right] \quad : \text{if } R \text{ is not dividable to } L \end{cases} \quad (23)$$

$$K = \sum_{n=1}^{y} \frac{1}{(1+ir)^{L \times n}} \quad (24)$$

In the above equations, ir is the discount rate and R is the useful life of the system.

2.7. Case Study

The geographical specifications of the study area, Khalkhal, Ardabil, Iran, are given in Table 2. The optimization problem examines the ability or inability of the composition obtained for the system, as well as the degree of reliability of the system in meeting consumer demand, which is shown in Fig. 3. These constraints are tested in all simulation steps and if not implemented in one step, the resulting combination is unsuitable and is removed from the possible designs.

Table 2. Geographical specifications of the study area

Location	Khalkhal, Ardabil, Iran
Latitude	+37.6205 N
Longitude	+48.5330 E
Altitude	2242 m

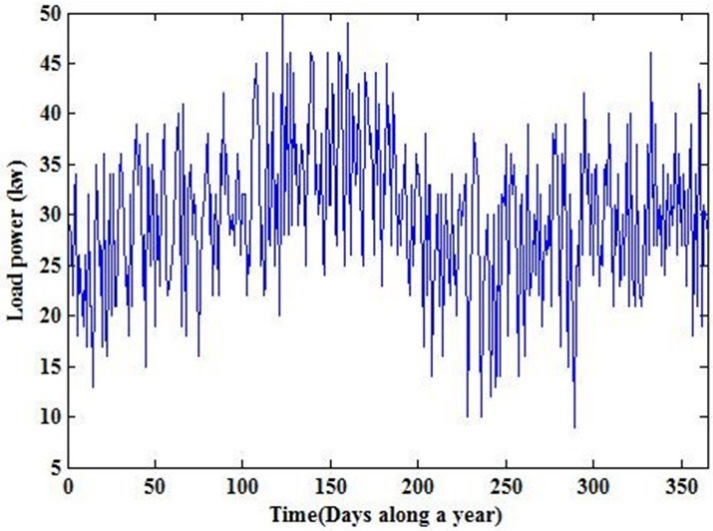

Fig. 3. Load consumption throughout the year [48]

According to Fig. 3, the peak electricity consumption of the site is related to the summer season. Therefore, the integrated system must be optimized to be able to supply the energy demand. According to studies on the region, on these days of the year, the region has suitable conditions for installing hydroelectric generators in the path of water transmission canals and also receiving suitable wind energy for installing wind turbines, and finally providing reliable energy required by the site during the year. Information about wind intensity in this region is obtained from the Renewable Energy and Energy Efficiency Organization (SATBA) [49] and applied in the simulation. This information is shown graphically in Fig. 4. The objective function of the problem is a hybrid model based on the cost of power plant construction and the reliability of the proposed system, which is calculated and presented by the ACO algorithm.

Information about water flow through the river located in the reference site and also values related to wind intensity are applied numerically at the beginning of the optimization problem. According to the figure 2, the output power of small wind and hydropower units is calculated in each simulation step and the load supply condition is checked at the same time. If the above condition is not satisfied in one iteration, the plan is removed from the existing plans, and the proposed algorithm searches for the optimal point of the problem with the aim of the lowest possible cost and also provides a reliable load under different weather conditions. The technical specifications and prices of the equipment used in this research are shown in Table 3 based on the new standards and the latest prices.

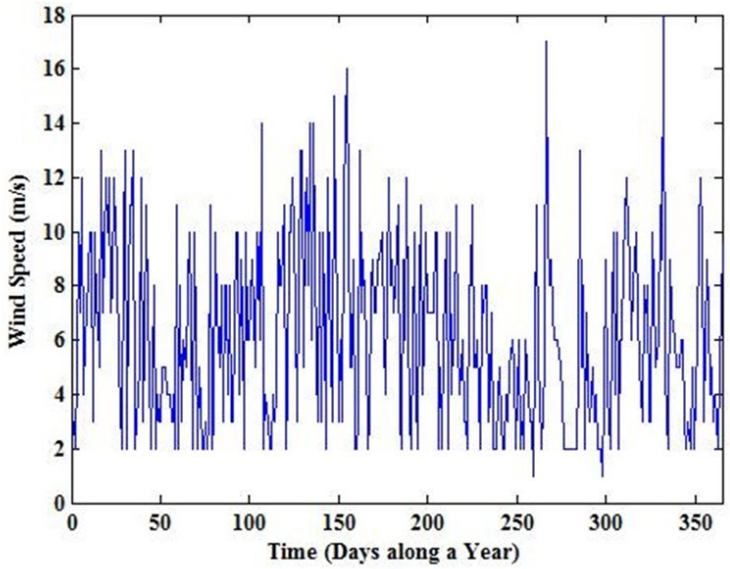

Fig. 4. Wind intensity in the study area [42]

Table 3. Technical specifications of the equipment used in the system

Equipment	Investment cost (%) ($/unit)	Replacement cost ($/unit)	Annual cost (maintenance) ($/unit.yr)	Life span (yr)	Accessibility (%)	Efficiency (%)
Hydropower system	6000	2000	100	20	--	60
WG wind turbines	19400	15000	75	20	96	--
Battery	600	560	20	5	100	90
DC/AC inverter	800	750	8	15	99.89	90

3. Results and Discussion

The proposed system is related to a remote village in Ardabil to supply a 50 kW load at peak consumption. To investigate the response or non-response of the proposed system to load demand during the year, an approximate reliability model has been used in this study. The total energy generated by the wind turbine and hydropower system is shown in Fig. 5.

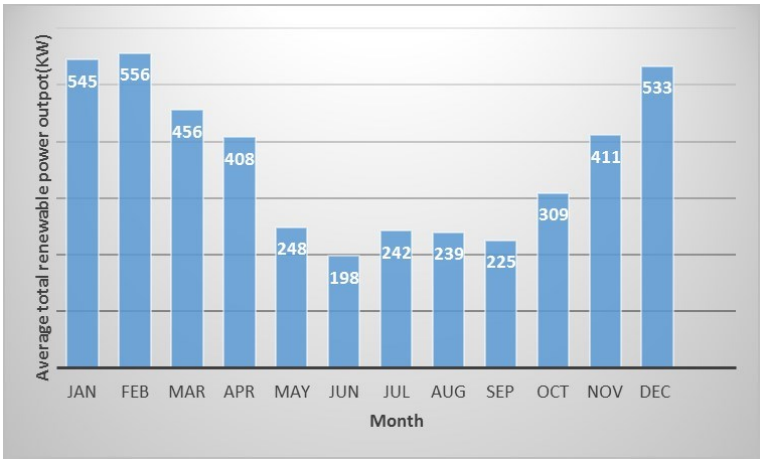

Fig. 5. Average total power generated by the system

As seen in Fig. 5, the lowest average of total energy production by wind turbines and hydropower turbines is related to the spring and summer months, whereby the lowest amount is related to June with an average of 198 kW. After June, September and August are on average with 225 and 235 kW, respectively. However, the highest average production for the studied system is related to the cold months of the year, winter and autumn, with the highest average in February, producing 556 kW, and June producing 545 kW of electricity. Fig. 6 shows the amount of electricity generated by a hydropower turbine.

According to Fig. 6, the highest amounts of electricity generation by turbines are related to the wet months of the year, spring and summer, specifically the highest average is related to September with 14.3 kW, while for this year the lowest average is related to December with 5.6 kW. To find the optimal composition of the proposed power plant, a MATLAB programming environment has been used .The program was performed with an initial population of 60 people and 200 iterations for the proposed algorithm and the optimal combination presented in Table 4.

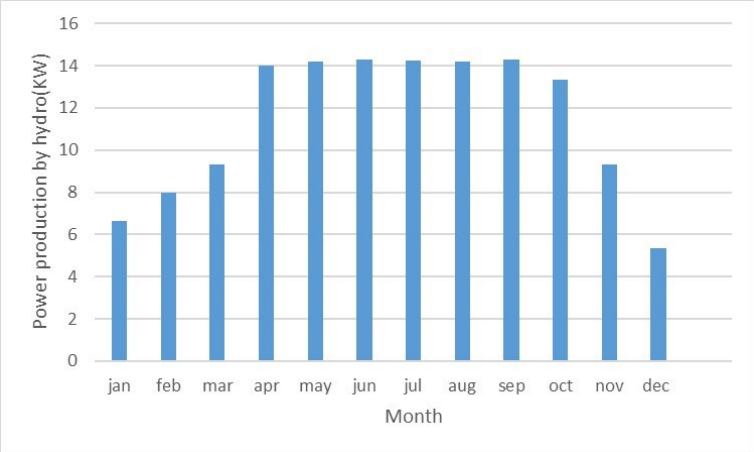

Fig. 6. Power is generated by the hydropower system

Table 4. Optimization results by ACO algorithm

Parameter	Number of Iteration	N_{WG}	N_{Batt}	P_{hydro}(kW)	Cost ($)
Results of the ACO algorithm	100	9	24	12.8	222538
1	120	12	26	12.2	236231
2	150	10	23	14.6	202138
3	200	13	19	11.6	239342
4	500	12	25	12.1	228967

According to the results of the hybrid system simulation, the proposed algorithm is implemented with different populations and the results were obtained in 5 stages of the simulation. The best solution was obtained in 150 iterations of the hybrid system simulation. For this case, to supply the required electric charge, it will need 10 wind turbines and 23 kVA batteries, as well as a 14.6 kW hydropower turbine, which will cost $ 202,138. According to the results, the accuracy of the ACO is corroborated and has a lower cost for the construction and operation of a combined system in the study area. Fig. 7 and Fig. 8 present the convergence process of the ACO considering the hydropower turbine and the hydropower turbine, respectively.

According to the results, the COE in the wind-hydropower system is gauged at 0.261 $/kWh battery storage. The studied system is implemented to provide a reliable load at peak time (50 kW) and with an optimal combination targeted at achieving the minimum cost of construction of the power plant. The obtained value is significantly high for system reliability and is suitable for implementing the system in the study area. It should be added that the system has a lifespan of 20 years and all prices are real and based on modern standards.

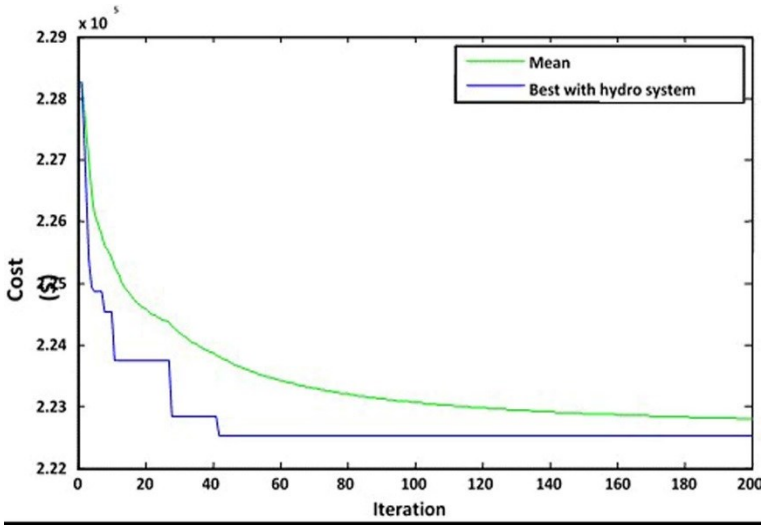

Fig. 7. Convergence process of the ACO with the hydropower turbine

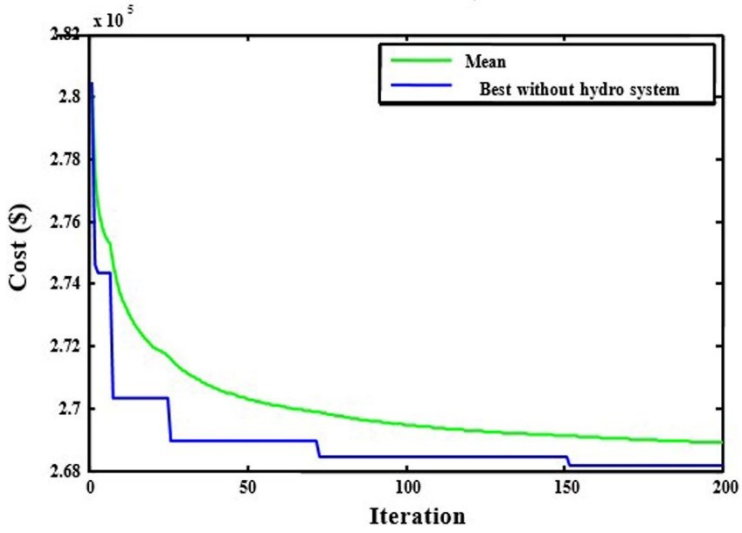

Fig. 8. Convergence process of the ACO regardless of the hydropower turbine

4. Conclusion

The main purpose of integrating small hydropower turbines with other energy sources is the reliability of the supply of electricity to remote villages under different weather conditions and, on the other hand, the reduction of construction and operation costs of the system. In this thread, the study examined the costs of a grid-independent wind-hydropower plant over 20 years. With a case study of a village in Ardabil, Iran. The river water flow in this area was measured at 146 L/s. The best waterfall height in this area was identified as 5 meters, which is the best point for installing a hydroelectric generator .In addition to the high reliability of the proposed system during the simulation process, the construction cost of the power plant is $ 45656 lower than the case without the use of a hydropower turbine, due to the cheaper hydropower system compared to wind turbines. The optimal combination of this power plant was achieved using the ACO algorithm. According to the results, the COE in the wind-hydropower system, with battery storage was obtained at 0.261 $/kWh. Therefore, adding a hydropower system resulted in reducing the total cost of constructing the system, augmenting the reliability of the system, and reducing the cost of energy production. The results of the simulation could be implemented in the study area by implementing the integrated wind and hydropower plant project at this site, while providing the necessary electricity from renewable and permanent sources, reducing the environmental pollution caused by the use of end-of-life fossil fuels.

Author Contribution: All authors contributed equally to the main contributor to this paper. All authors read and approved the final paper.

Funding: No funding for this research.

Conflicts of Interest: The authors declare no conflict of interest.

References

[1] R. M. Elavarasan *et al.,* "COVID-19: Impact analysis and recommendations for power sector operation," *Applied energy*, vol. 279, p. 115739, 2020, https://doi.org/10.1016/j.apenergy.2020.115739.

[2] A. Aldegheishem, M. Anwar, N. Javaid, N. Alrajeh, M. Shafiq, and H. Ahmed. "Towards Sustainable Energy Efficiency With Intelligent Electricity Theft Detection in Smart Grids Emphasising Enhanced Neural Networks," *IEEE Access*, vol. 9, pp. 25036–25061, 2021, https://doi.org/10.1109/access.2021.3056566.

[3] M. Jahangiri, A. Haghani, S. Heidarian, A. Mostafaeipour, H. A. Raiesi and A. Alidadi Shamsabadi, "Sensitivity analysis of using solar cells in regional electricity power supply of off-grid power systems in Iran," *Journal of Engineering, Design and Technology*, vol. 18, no. 6, pp. 1849-1866, 2020, https://doi.org/10.1108/JEDT-10-2019-0268.

[4] S. Makhdoomi and A. Askarzadeh, "Optimizing operation of a photovoltaic/diesel generator hybrid energy system with pumped hydro storage by a modified crow search algorithm," *Journal of Energy Storage*, vol. 27, p. 101040, 2020, https://doi.org/10.1016/j.est.2019.101040.

[5] Y. Cao, M. Delpisheh, S. Yousefiasl, H. Athari, M. A. El-Shorbagy, F. Jarad, M. Dahari, and M. Waehayee. "Examination and optimization of a novel auxiliary trigeneration system for a ship through waste-to-energy from its engine," *Case Stud Therm Eng*, vol. 31, p. 101860, 2022, https://doi.org/10.1016/J.CSITE.2022.101860.

[6] R. Alayi, R. Kumar, S. R. Seydnouri, M. H. Ahmadi, and A. Issakhov. "Energy, environment and economic analyses of a parabolic trough concentrating photovoltaic/thermal system," *Int J Low-Carbon Technol*, vol. 16, pp. 570–576, 2020, https://doi.org/10.1093/ijlct/ctaa086.

[7] R. Alayi, N. Khalilpoor, S. Heshmati, A. Najafi, and A. Issakhov. "Thermal and Environmental Analysis Solar Water Heater System for Residential Buildings," *Int J Photoenergy,* pp. 1–9, 2021, https://doi.org/10.1155/2021/6838138.

[8] C. W. Forsberg, B. E. Dale, D. S. Jones, T. Hossain, A. R. C. Morais, and L. M. Wendt. "Replacing liquid fossil fuels and hydrocarbon chemical feedstocks with liquid biofuels from large-scale nuclear biorefineries," *Appl Energy*, vol. 298, p. 117225, 2021, https://doi.org/10.1016/j.apenergy.2021.117225.

[9] M. Hekmatshoar, M. Deymi-Dashtebayaz, M. Gholizadeh, D. Dadpour, and M. Delpisheh. "Thermoeconomic analysis and optimization of a geothermal-driven multi-generation system producing power, freshwater, and hydrogen," *Energy,* vol. 247, p. 123434, 2022, https://doi.org/10.1016/J.ENERGY.2022.123434.

[10] M. Delpisheh, M. A. Haghghi, H. Athari, and M. Mehrpooya. "Desalinated water and hydrogen generation from seawater via a desalination unit and a low temperature electrolysis using a novel solar-based setup," *Int J Hydrogen Energy*, vol. 46, pp. 7211–7229, 2021, https://doi.org/10.1016/j.ijhydene.2020.11.215.

[11] M. Delpisheh, M. Abdollahi Haghghi, and M. Mehrpooya, A. Chitsaz, and H. Athari. "Design and financial parametric assessment and optimization of a novel solar-driven freshwater and hydrogen cogeneration system with thermal energy storage," *Sustain Energy Technol Assessments,* vol. 45, p. 101096, 2021, https://doi.org/10.1016/j.seta.2021.101096.

[12] T. S. Adebayo, H. Rjoub, G. D. Akinsola, and S. D. Oladipupo. "The asymmetric effects of renewable energy consumption and trade openness on carbon emissions in Sweden: new evidence from quantile-on-quantile regression approach," *Environ Sci Pollut Res,* vol. 29, pp. 1875–1886, 2021, https://doi.org/10.1007/s11356-021-15706-4.

[13] T. S. Adebayo, M. F. Coelho, D. Ç. Onbaşıoğlu, H. Rjoub, M. N. Mata, P. V. Carvalho, J. X. Rita, and I. Adeshola, "Modeling the Dynamic Linkage between Renewable Energy Consumption, Globalization,

and Environmental Degradation in South Korea: Does Technological Innovation Matter?," *Energies*, vol. 14, p. 4265, 2021, https://doi.org/10.3390/en14144265.

[14] E. Assareh, M. Delpisheh, E. Farhadi, W. Peng, and H. Moghadasi. "Optimization of geothermal- and solar-driven clean electricity and hydrogen production multi-generation systems to address the energy nexus," *Energy Nexus,* vol. 5, p. 100043, 2022, https://doi.org/10.1016/J.NEXUS.2022.100043.

[15] T. S. Adebayo, and H. Rjoub. "A new perspective into the impact of renewable and nonrenewable energy consumption on environmental degradation in Argentina: a time–frequency analysis," *Environ Sci Pollut Res*, vol. 29, pp. 16028–16044, 2021, https://doi.org/10.1007/s11356-021-16897-6.

[16] W. Zhang, A. Maleki, F. Pourfayaz, and M. S. Shadloo. "An artificial intelligence approach to optimization of an off-grid hybrid wind/hydrogen system," *Int J Hydrogen Energy*, vol. 46, pp. 12725–12738, 2021, https://doi.org/10.1016/j.ijhydene.2021.01.167.

[17] L. Lander, E. Kallitsis, A. Hales, J. S. Edge, A. Korre, and G. Offer. "Cost and carbon footprint reduction of electric vehicle lithium-ion batteries through efficient thermal management," *Appl Energy,* vol. 289, p. 116737, 2021, https://doi.org/10.1016/j.apenergy.2021.116737.

[18] G. Gasore, H. Ahlborg, E. Ntagwirumugara, and D. Zimmerle. "Progress for On-Grid Renewable Energy Systems: Identification of Sustainability Factors for Small-Scale Hydropower in Rwanda," *Energies,* vol. 14, p. 826, 2021, https://doi.org/10.3390/en14040826.

[19] N. Ravichandran, N. Ravichandran, and B. Panneerselvam. "Performance analysis of a floating photovoltaic covering system in an Indian reservoir," *Clean Energy*, vol. 5, pp. 208–228, 2021, https://doi.org/10.1093/ce/zkab006.

[20] S. Rawas. "Energy, network, and application-aware virtual machine placement model in SDN-enabled large scale cloud data centers," *Multimed Tools Appl,* vol. 80, pp. 15541–15562, 2021, https://doi.org/10.1007/s11042-021-10616-6.

[21] I. F. G. Reis, I. Gonçalves, M. A. R. Lopes, and C. H. Antunes. "Assessing the Influence of Different Goals in Energy Communities' Self-Sufficiency—An Optimized Multiagent Approach," *Energies,* vol. 14, p. 989, 2021, https://doi.org/10.3390/en14040989.

[22] T. Parikhani, M. Delpisheh, M. A. Haghghi, S. G. Holagh, and H. Athari. "Performance enhancement and multi-objective optimization of a double-flash binary geothermal power plant," *Energy Nexus,* p. 100012, 2021, https://doi.org/10.1016/J.NEXUS.2021.100012.

[23] P. Matrenin, M. Safaraliev, S. Dmitriev, S. Kokin, B. Eshchanov, and A. Rusina. "Adaptive ensemble models for medium-term forecasting of water inflow when planning electricity generation under climate change," *Energy Reports,* vol. 8, pp. 439–447, 2022, https://doi.org/10.1016/j.egyr.2021.11.112.

[24] H. Liu, B. Wu, A. Maleki, F. Pourfayaz, and R. Ghasempour. "Effects of Reliability Index on Optimal Configuration of Hybrid Solar/Battery Energy System by Optimization Approach: A Case Study," *Int J Photoenergy,* pp. 1–11, 2021, https://doi.org/10.1155/2021/9779996.

[25] A. Maleki. "Optimization based on modified swarm intelligence techniques for a stand-alone hybrid photovoltaic/diesel/battery system," *Sustain Energy Technol Assessments,* vol. 51, p. 101856, 2022, https://doi.org/10.1016/j.seta.2021.101856.

[26] S. A. Mousavi, M. Mehrpooya, and M. Delpisheh. "Development and life cycle assessment of a novel solar-based cogeneration configuration comprised of diffusion-absorption refrigeration and organic Rankine cycle in remote areas," *Process Saf Environ Prot*, vol. 159, pp. 1019–1038, 2022, https://doi.org/10.1016/J.PSEP.2022.01.067.

[27] N. Mughal, A. Arif, V. Jain, S. Chupradit, M. S. Shabbir, C. S. Ramos-Meza, and R. Zhanbayev. "The role of technological innovation in environmental pollution, energy consumption and sustainable economic growth: Evidence from South Asian economies," *Energy Strateg Rev*, vol. 39, p. 100745, 2022, https://doi.org/10.1016/j.esr.2021.100745.

[28] T. S. Kishore, E. R. Patro, V. Harish VSK, and A. T. Haghighi. "A Comprehensive Study on the Recent Progress and Trends in Development of Small Hydropower Projects," *Energies,* vol. 14, p. 2882, 2021, https://doi.org/10.3390/en14102882.

[29] L. Zhang, M. Pang, A. S. Bahaj, Y. Yang, and C. Wang. "Small hydropower development in China: Growing challenges and transition strategy," *Renew Sustain Energy Rev,* vol. 137, p. 110653, 2021, https://doi.org/10.1016/j.rser.2020.110653.

[30] X. Ren, Y. Wu, D. Hao, G. Liu, and N. Zafetti. "Analysis of the performance of the multi-objective hybrid hydropower-photovoltaic-wind system to reduce variance and maximum power generation by developed owl search algorithm," *Energy,* vol. 231, p. 120910, 2021, https://doi.org/10.1016/J.ENERGY.2021.120910.

[31] L. Lu, W. Yuan, C. Su, P. Wang, C. Cheng, D. Yan, and Z Wu. "Optimization model for the short-term joint operation of a grid-connected wind-photovoltaic-hydro hybrid energy system with cascade hydropower plants," *Energy Convers Manag,* vol. 236, p. 114055, 2021, https://doi.org/10.1016/J.ENCONMAN.2021.114055.

[32] Q. Tan, X. Wen, Y. Sun, X. Lei, Z. Wang, and G. Qin. "Evaluation of the risk and benefit of the complementary operation of the large wind-photovoltaic-hydropower system considering forecast uncertainty," *Appl Energy,* vol. 285, p. 116442, 2021, https://doi.org/10.1016/J.APENERGY.2021.116442.

[33] S. Sterl, P. Donk, P. Willems, and W. Thiery. "Turbines of the Caribbean: Decarbonising Suriname's electricity mix through hydro-supported integration of wind power," R*enew Sustain Energy Rev,* vol. 134, pp. 110352, 2020, https://doi.org/10.1016/J.RSER.2020.110352.

[34] Y. Zhang, J. Lian, C. Ma, Y. Yang, X. Pang, and L. Wang. "Optimal sizing of the grid-connected hybrid system integrating hydropower, photovoltaic, and wind considering cascade reservoir connection and photovoltaic-wind complementarity," *J Clean Prod*, vol. 274, p. 123100, 2020, https://doi.org/10.1016/J.JCLEPRO.2020.123100.

[35] M. Zhao, Y. Wang, X. Wang, J. Chang, Y. Chen, Y. Zhou, and A. Guo. "Flexibility evaluation of wind-PV-hydro multi-energy complementary base considering the compensation ability of cascade hydropower stations," *Appl Energy,* vol. 315, p. 119024, 2022, https://doi.org/10.1016/J.APENERGY.2022.119024.

[36] E. Assareh, M. Delpisheh, S. M. Alirahmi, S. Tafi, and M. Carvalho. "Thermodynamic-economic optimization of a solar-powered combined energy system with desalination for electricity and freshwater production," *Smart Energy,* vol. 5, p. 100062, 2022. https://doi.org/10.1016/J.SEGY.2021.100062.

[37] C. Ammari, D. Belatrache, B. Touhami, S. Makhloufi. "Sizing, optimization, control and energy management of hybrid renewable energy system—A review," *Energy Built Environ*, 2021, https://doi.org/10.1016/j.enbenv.2021.04.002.

[38] P. Cabrera, J. A. Carta, H. Lund, and J. Z. Thellufsen. "Large-scale optimal integration of wind and solar photovoltaic power in water-energy systems on islands," *Energy Convers Manag,* vol. 235, p. 113982, 2021, https://doi.org/10.1016/j.enconman.2021.113982.

[39] J. Yan, O. A. Broesicke, X. Tong, D. Wang, D. Li, and J. C. Crittenden. "Multidisciplinary design optimization of distributed energy generation systems: The trade-offs between life cycle environmental and economic impacts," *Appl Energy,* vol. 284, p. 116197, 2021, https://doi.org/10.1016/j.apenergy.2020.116197.

[40] N. M. Eshra, A. F. Zobaa, and S. H. E. Abdel Aleem. "Assessment of mini and micro hydropower potential in Egypt: Multi-criteria analysis," *Energy Reports*, vol. 7, pp. 81–94, 2021, https://doi.org/10.1016/j.egyr.2020.11.165.

[41] R. Alayi, F. Zishan, S. R. Seyednouri, R. Kumar, M. H. Ahmadi, and M. Sharifpur. "Optimal Load Frequency Control of Island Microgrids via a PID Controller in the Presence of Wind Turbine and PV," *Sustainability,* vol. 13, p. 10728, 2021, https://doi.org/10.3390/su131910728.

[42] P. G. Anselma, M. Del Prete, and G. Belingardi. "Battery High Temperature Sensitive Optimization-Based Calibration of Energy and Thermal Management for a Parallel-through-the-Road Plug-in Hybrid Electric Vehicle," *Appl Sci*, vol. 11, p. 8593, 2021, https://doi.org/10.3390/app11188593.

[43] R. Alayi, M. Jahangiri, J. W. G. Guerrero, R. Akhmadeev, R. A. Shichiyakh, and S. A. Zanghaneh. "Modelling and reviewing the reliability and multi-objective optimization of wind-turbine system and photovoltaic panel with intelligent algorithms," *Clean Energy,* vol. 5, pp. 713–730, 2021, https://doi.org/10.1093/ce/zkab041.

[44] J. López-Marín, A. Gálvez, F. M. del Amor, and J. M. Brotons. "The Financial Valuation Risk in Pepper Production: The Use of Decoupled Net Present Value," *Math,* vol. 9, 2021, https://doi.org/10.3390/math9010013.

[45] E. Jadidi, M. H. K. Manesh, M. Delpisheh, and V. C. Onishi. "Advanced Exergy, Exergoeconomic, and Exergoenvironmental Analyses of Integrated Solar-Assisted Gasification Cycle for Producing Power and Steam from Heavy Refinery Fuels," *Energies,* vol. 14, p. 8409, 2021, https://doi.org/10.3390/EN14248409.

[46] H. Athari, F. Kiasatmanesh, M. A. Haghghi, F. Teymourzadeh, H. Yagoublou, and M. Delpisheh. "Investigation of an auxiliary option to meet local energy demand via an innovative small-scale geothermal-driven system; a seasonal analysis," *J Build Eng*, p. 103902, 2021, https://doi.org/10.1016/J.JOBE.2021.103902.

[47] S. M. Alirahmi, E. Assareh, N. N. Pourghassab, M. Delpisheh, L. Barelli, and A. Baldinelli, "Green hydrogen & electricity production via geothermal-driven multi-generation system: Thermodynamic modeling and optimization," *Fuel*, vol. 308, p. 122049, 2022, https://doi.org/10.1016/J.FUEL.2021.122049.

[48] Iran power generation and transmission company (Tavanir) 2022. https://www.tavanir.org.ir/ (accessed April 28, 2022).

[49] Renewable Energy and Energy Efficiency Organization (Satba) 2022. http://www.satba.gov.ir (accessed April 28, 2022).